STRUCTURAL, OPTICAL AND ELECTRICAL PROPERTIES OF TIN DOPED IN$_2$O$_3$ THIN FILMS PREPARED BY SPRAY ULTRASONIC

N. HAMANI, A. ATTAF*, H. SAIDI, K. BENNACEUR, N. MESSEI

Physics of Thin Films and Applications Laboratory (LPCMA), University of Biskra, BP 145 RP, Biskra 07000, Algeria

ab_attaf@yahoo.fr, ab_attaf@univ-biskra.dz

ABSTRACT

Indium tin oxide (ITO) thin films have been prepared by ultrasonic spray pyrolysis technique using different Sn concentrations on a glass substrate at 400°C. X-ray diffraction patterns reveal that all films have polycrystalline cubic structure with preferentially oriented along (400) plane. The films high optical transmittance is improved from 70 % to 80 % in visible region and optical band gap is increased from 3.69 to 3.84 eV with increasing tin concentration. The electrical measurements were performed using four probes technique. The maximum value of conductivity is 813 (Ω.cm)$^{-1}$ was measured in 8% Sn doped film.

KEYWORDS: In$_2$O$_3$; Thin films; Sn doping; Ultrasonic spray method.

1 INTRODUCTION

During the last two decades, the dominant transparent conducting oxides (TCOs) have been tin oxide (SnO$_2$) indium oxide (In$_2$O$_3$), indium tin oxide (In$_2$O$_3$:Sn or ITO), and zinc oxide (ZnO), which have found applications in wide areas such as electronic and optoelectronic fields.

Stoichiometric In$_2$O$_3$ is a well-known to be a transparent intrinsic semiconductor that can be doped by substituting indium (In) atoms by tin (Sn) ones yielding indium tin oxide (ITO) [1]. Due to the high transmittance in the visible spectral region and the high conductivity, indium tin oxide films found a wide interest. Thereafter, the broad applications of ITO in electronic and optical devices such as: transparent electrodes for display devices, gas sensors, heating elements [2]. For these applications, the typical characteristics required are: an electrical resistivity lower than 1×10^4 (Ω.cm) [3-6] and an optical transmittance higher than 80 % in the visible spectrum [4.7]. Indium tin oxide thin-films have been deposited using various methods, such as magnetron sputtering [8-9], sol–gel deposition [10], electron beam evaporation [11], chemical vapor deposition [12], pulsed laser deposition [13], and spray pyrolysis [14 -16]. Spray pyrolysis is one of the most popular techniques due to its low cost, in addition, it can operate in atmospheric pressure, and it is suitable for large-scale coating.

In the present work, we have deposited tin doped In2O3 thin films deposited on glass substrates at 400°C by ultrasonic spray technique to study its opto-electrical properties, and crystal structure.

2 EXPERIMENTAL DETAILS

In the present work, Indium tin oxide films are prepared using a ultrasonic spray deposition system (Fig. 1). In$_2$O$_3$:Sn solution were prepared by dissolving 0.1 M indium chloride hydrate (InCl$_3$, 4H$_2$O) was used as the source of Indium source ,dissolved in an appropriate amount of methanol CH$_3$OH solution (99.995%) purity and Tin chloride hydrate SnCl$_4$.5H$_2$O (99.0%) was used as tin (Sn) doped . Some drops of HCl solution have been added as stabilizer. The tin doping level in the solution was varied from 0 to 10 at% on glass substrates heated at 400°C in atmospheric pressure. All Substrates were cleaned and degreased successively using Acetone, propanol, and distilled water. The solution flow rate was chosen to be 50 mL/h. Films structure was analyzed using X-ray spectroscopy on a D8 ADVANCE Diffract meter by a Cu Kα radiation ($\lambda = 1.5405$ Å), the optical transmittance spectra were obtained by a UV–VIS spectrophotometer. These measurements were carried using glass as reference in a wavelength range of 200–800 nm. Electrical resistivity was measured by four-point method.

Table 01: Deposition Parameters

Doping level (at %)	Amount of solution (ml)	Substrate temperature (°C)	Deposition time (min)	Distance Nozzle -substrate (cm)
Undoped	40	400	5	4.5
2	/	/	/	/
4	/	/	/	/
6	/	/	/	/
8	/	/	/	/
10	/	/	/	/

Figure 01: Schematic diagram of the ultrasonic spray technique

3   RESULTS AND DISCUSSION

3.1   Structural studies

Fig. 2 shows the X-ray diffraction patterns of indium tin oxide thin films prepared with different tin concentrations. This result shows that all films have polycrystalline structure; they crystallize in the cubic bixyite structure of indium In_2O_3. The obtained phase was in accordance with the standard JCPDS data (Card no. 65-3170) [17]. As can be seen, the whole films have a preferential orientation in the plane (400) around the angle $2\theta = 35.62°$. The increasing intensity of the (400) plane is attributed to the increase of crystallite size and growth along this plane.

The crystallite size was calculated from the XRD pattern using Debye-Scherrer formula [18-20]:

$$D = \frac{0,9.\lambda}{\beta.\cos\theta}$$

(1)

Where λ is X-ray wavelength (λ = 1.54060°A), β is full width at half maximum in radian and θ is Bragg's angle. The dislocation density (δ) and strain (ε) was calculated using the following equations [18]:

$$\delta = \frac{1}{D^2}$$

(2)

$$\varepsilon = \frac{a - a_1}{a_1} \times 100\%$$

(3)

Structural parameters of prepared ITO thin films using the above equations are presented in Table 2. The variation of crystallite size and strain with doping concentration are reported in Fig. 3. The crystallite size enhances with films doping. The increase in the crystallite size from 49.2 to 59 nm is caused by coalescence of crystallites during films growth.

The strain and dislocation density of (400) planes are given in Table 1. The calculated value of lattice constant of prepared ITO films are a= 10,0615A° to 10, 0899A°, they are slightly smaller than the reported value 10.118 A° for pure indium oxide (JCPDS Card No. 06-0416). This can be attributed to the oxygen deficiency [21].
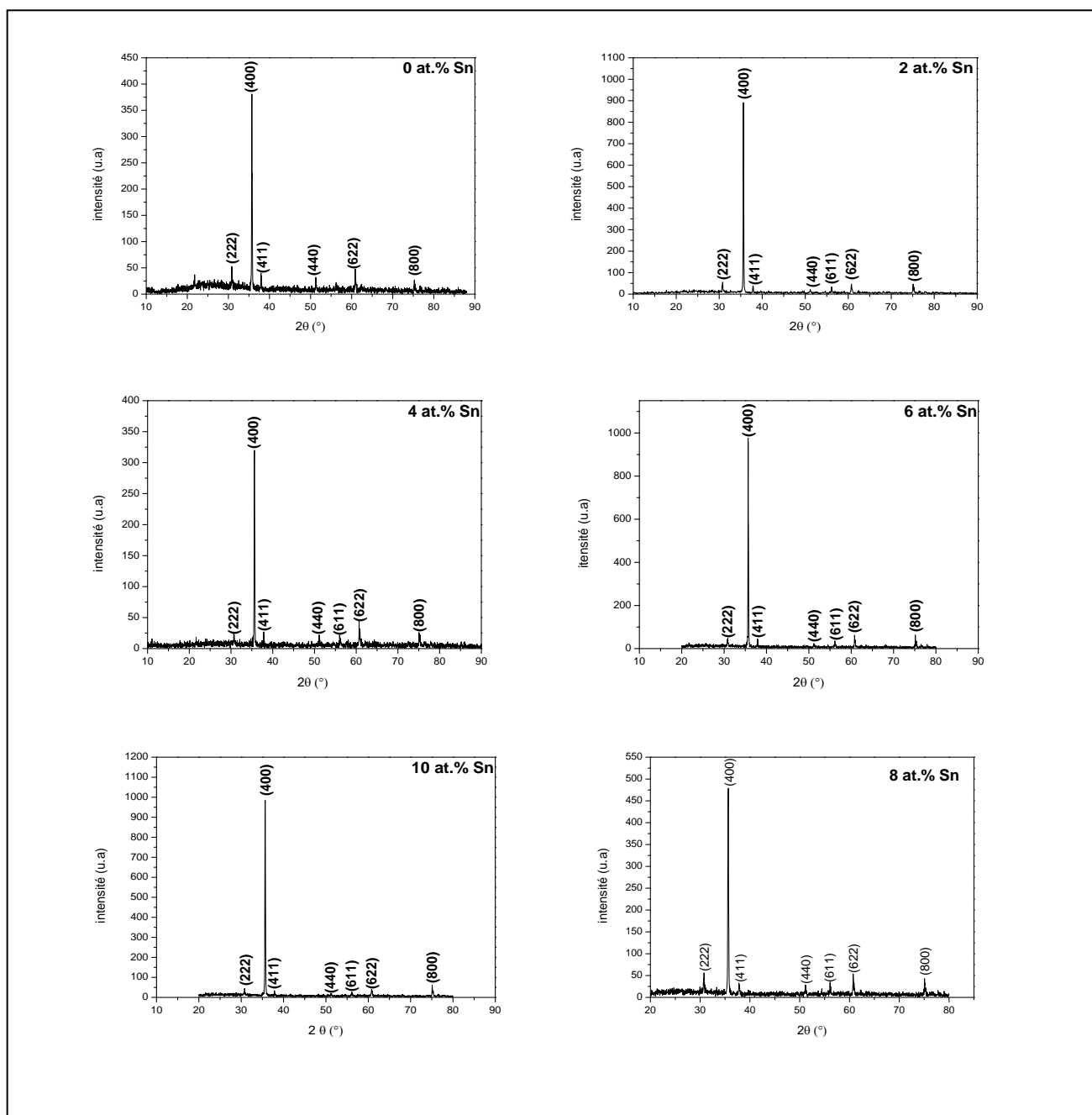
Figure 02: X-ray pattern of Indium tin oxide films prepared at various concentrations

Table 02: Structural parameters of prepared indium tin oxide (ITO) thin films for different Sn concentrations

	2θ (°)	FWHM (°)	d-spase (A°)	hkl	Crystallite size (nm)	a(A°)	ε%	δ (×10^{14}lignes/m^2)
Undoped	35,6948	0,1771	2,51543	400	49,201	10,0615	−0,4797	4,1310
2	35,6346	0,2066	2,51954	400	42,168	10,0779	−0,3175	5,6238
4	35,5908	0,1771	2,52254	400	49,186	10,0899	−0,1988	4,1335
6	35,6708	0,1476	2,51707	400	59,030	10,0680	−0,4154	2,8698

8	35,6301	0,1771	2,51985	400	49,192	10,0792	−0,3046	4,1325
10	35,6434	0,1476	2,51894	400	59,026	10,0755	−0,3412	2,8702
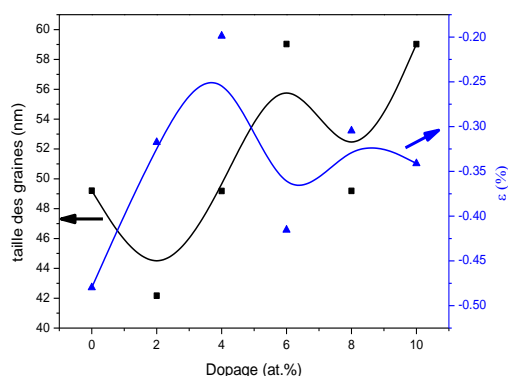
Figure 03: Variation of grain size and strain of indium tin oxide with Sn concentration

3.2 Optical studies

The optical properties of thin films are known to depend strongly on the films thickness, microstructures, levels of impurities and deposition parameters. The optical transmittance of prepared indium tin oxide (ITO) thin films for different doping concentrations is shown in Fig. 4. It can be seen that the average transmittance of the tin doped indium oxide film is 85% at 8 % Sn. Films optical transmission spectra after doping, indicates a highly transparent material (>80%) in the visible range. the large films absorbance in the interval 300< λ< 400 nm due to the excitation and electrons migration from the valence band to the conduction band.
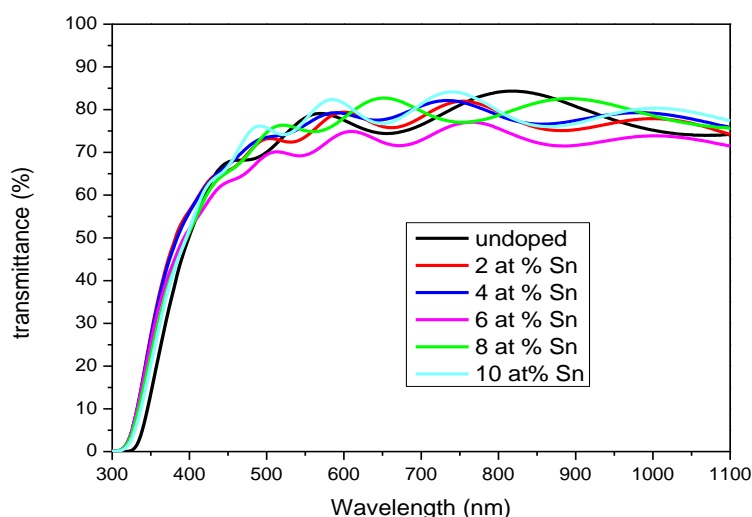
Figure 04: Transmittance spectra of the indium tin oxide thin films as a function of Sn doping

The direct optical band gap energy E_g of ITO films was calculated from the transmission spectra using the following relations [18].

$$(\alpha h\upsilon)^2 = A(h\upsilon - Eg) \qquad (4)$$

Where α is absorption coefficient, A is the constant independent of photon energy (hυ), and Eg is the optical band gap. The values of optical band gap are illustrated in fig 5.

It is observed that band gap increaυses rapidly from 3,69 (0 at %) to 3,84eV (8at%) and then decreased slightly to 3,80eV (10 at%). A Similar behavior of band gap, for high tin doping, is reported previously by Benamar et al [22]. The widening of the optical band gap is related to increased carrier concentration, which is explained in terms of Moss–Burstein effect [17]. The narrowing of band gap for higher Sn doping may be due to many-body interaction effects either between free carriers or between free carriers and ionized impurities [23].

24
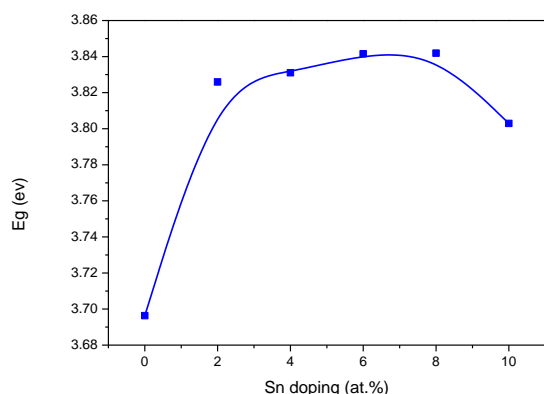
Figure 05: Variations of optical band gap of indium tin oxides thin films as function of Sn concentrations

3.3 Electrical studies

The measured electrical parameters of prepared ITO thin films, are showed in Fig. 6. As can be seen, the resistivity is decreased with increasing Sn concentrations; this is desirable for transparent conducting oxide. The results indicate that the prepared ITO thin films are highly degenerating n-type conductivity [5]. The incorporation of Sn dopant in indium oxide films changes the overall electrical film properties significantly. We obtained a minimum electrical resistivity $3.9 \times 10^{-4}(\Omega.cm)$. Similar results were reported in previous literature by Seki et al[17]. The mobility increase is related to the reduction of grain boundary scattering. The electronic transport property for films is entirely related to the films microstructure and doping concentration.
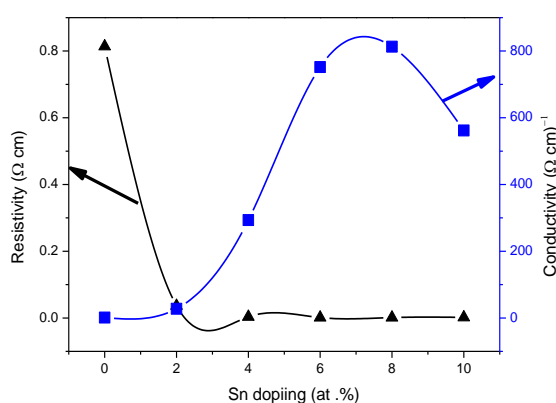
Figure 06: Electrical parameters of prepared indium tin oxide ITO thin films as function of Sn concentrations.

4 CONCLUSIONS

In this work, we have optimized the doping ratio of tin-doped In$_2$O$_3$ films prepared by reactive spray ultrasonic

pyrolysis. The obtained results indicated that films ITO have a good crystallinity and exhibit cubic structure with a preferential orientation along (4 0 0) direction. In addition, the optical study shows transmission exceeding 85% in the visible region and a high absorption in the IR region. The films optical gap varies from 3.69 to 3.84 eV. The film prepared at 8 at % showed lower value of electrical resistivity (ρ).These results suggest that the prepared films may have applications in optoelectronic devices production.

REFERENCES

[1] D. Raoufi, L. Eftekhari, Surface & Coatings Technology, 274 (2015) 44–50.

[2] A. Kachouane, M. Addoua, A. Bougrine, B. El idrissi , R. Messoussi, M. Regragui, J.C. Bérnede, Materials Chemistry and Physics, 70 (2001) 285–289.

[3] G.H. Takaoka, D. Yamazaki, J. Matsuo , Materials Chemistry and Physics, 74 (2002) 104–108.

[4] A. El Hichou, A. Kachouane, J.L. Bubendorff, M. Addou, J. Ebothe, M.T. Royon, A. Bougrine, Thin Solid Films, 458 (2004) 263–268.

[5] N.G. Pramod, S.N. Pandey, P.P. Sahay , Ceramics International 38 (2012) 4151–4158.

[6] A. Pokaipisit, M. Horprathum and Pichet Limsuwan, Songklanakarin J. Sci. Technol, 31 (5) (2009).

[7] C.W.O. Yang, H. Yeom , D. C. Paine , Thin Solid Films, 516 (2008) 3105–3111

[8] M. Ait Aouaj, R. Diaz, A. Belayachi, F. Rueda, M. Abd-Lefdil, Materials Research Bulletin, 44 (2009) 1458–1461.

[9] P. Prathap, Y.P.V. Subbaiah, M. Devika, K.T. R. Reddy, Materials Chemistry and Physics, 100 (2006) 375–379.

[10] C. Luangchaisri. S. Dumrongrattana, P. Rakkwamsuk, Procedia Engineering, 32 (2012) 663 – 669

[11] H. Bendjedidi, A. Attaf, H. Saidi, M. S. Aida, S. Semmari, A. Bouhdjar, Y. Benkhetta, Journal of Semiconductors, Vol. 36, No. 12 (2012)

[12] I. B. Kherkhachi, A. Attaf, H. Saidi, A. bouhdjar, H. Bendjdidi, Y. Benkhetta, R. Azizi, M.S. Aida,Optik, 127 (2016) 2266–2270

[13] Y. Lingmin, F. Xinhui, Q. Lijun, M. Lihe, Y. Wen, Applied Surface Science, 257 (2011) 3140–3144

[14] Y. Huang, G. Li, J. Feng, Q. Zhang, Thin Solid Films, 518 (2010) 1892–1896

[15] D.L. Zhang, L. Tao, Z.B. Deng, J.B. Zhang, L.Y. Chen, Mater. Chem. Phys. 100 (2006) 275.

[16] S. Kaleemulla, A. S. Reddy, S. Uthanna, P. S. Reddy, Journal of Alloys and Compounds, 479 (2009) 589–593

[17] M. Thirumoorthi, J. Thomas, J. Prakash , Journal of Asian Ceramic Societies, 4 (2016) 124–132.

[18] A. Attaf, A. Bouhdjer , H. Saidi, M.S. Aida, N. Attaf, H. Ezzaoui, Thin Solid Films, 625 (2017) 177–179.

[19] A. Bouhdjer, A. Attaf, H. Saidi , Y. Benkhetta, M.S. Aida, I. Bouhaf, A. Rhil, , Optik 127 (2016) 6329–6333.

[20] S. Benramache , B. Benhaoua, Superlattices and Microstructures, 52 (2012) 1062–1070.

[21] V.G. Rajeshmon, M.R. Rajesh Menon, C. Sudha Kartha, K.P. Vijayakumar, Journal of Analytical and Applied Pyrolysis 110 (2014) 448–454.

[22] E. Benamar, M. Rami, C. Messaoudi, D. Sayah, A. Ennaoui, Sol. Energy Mater.Sol. Cells, 56, 125–139 (1999).

[23] A. Walsh, J.L.F. Da Silva, S.-H. Wei, Phys. Rev. B, 78, 075211 (2008).